Effects of Fe-S-As coupled redox processes on arsenic mobilization in shallow aquifers of Datong Basin, northern China[☆]

Junwen Zhang [a, b], Teng Ma [a, *], Yani Yan [c], Xianjun Xie [a], Olusegun K. Abass [d], Congqiang Liu [b], Zhiqi Zhao [b], Zhizhen Wang [a]

[a] School of Environmental Studies, State Key Laboratory of Biogeology and Environmental Geology, China University of Geosciences, Wuhan, 430071, China
[b] State Key Laboratory of Environmental Geochemistry, Institute of Geochemistry, Chinese Academy of Sciences, Guiyang, 550002, China
[c] College of Environmental Science and Engineering, Guilin University of Technology, Guilin, 541004, China
[d] University of Chinese Academy of Sciences, Beijing 100049, Institute of Urban Environment, Chinese Academy of Sciences, Xiamen, 361021, China

ARTICLE INFO

ABSTRACT

High arsenic groundwater generally coexists with elevated Fe^{2+} concentrations (mg L^{-1} levels) under reducing conditions, but an explanation for the extremely high arsenic (up to ~2690) concentrations at very low Fe^{2+} (i.e., µg L^{-1} levels) in groundwater of Datong Basin remains elusive. Field groundwater investigation and laboratory microcosm experiments were implemented in this study. The field groundwater was characterized by weakly alkaline (pH 7.69 to 8.34) and reducing conditions (Eh −221.7 to −31.9 mV) and arsenic concentration averages at 697 µg L^{-1}. *Acinetobacter* (5.9–51.3%), *Desulfosporosinus* (4.6–30.2%), *Brevundimonas* (3.9–19%) and *Pseudomonas* (3.2–14.6%) were identified as the dominant genera in the bacterial communities. Bacterially mediated arsenate reduction, Fe(III) reduction, and sulfate reduction are processes occurring (or having previously occurred) in the groundwater. Results from incubation experiment (27 d) revealed that nitrate, arsenate, and Fe(III)/sulfate reduced sequentially with time under anoxic conditions, while Fe(III) and sulfate reduction processes had no obvious differences, occurring almost simultaneously. Moreover, low Fe^{2+} concentrations were attributed to initially high pH conditions, which relatively retarded Fe(III) reduction. In addition, arsenic behavior in relation to groundwater redox conditions, matrices, and solution chemistry were elaborated. Bacterial arsenate reduction process proceeded before Fe(III) and sulfate reduction in the incubation experiment, and the total arsenic concentration (dominated by arsenite) gradually increased from ~7 to 115 µg L^{-1} as arsenate was reduced. Accordingly, bacterially mediated reductive desorption of arsenate is identified as the main process controlling arsenic mobility, while Fe(III) reduction coupled with sulfate reduction are secondary processes that have also contributed to arsenic enrichment in the study site. Overall, this study provide important insights into the mechanism controlling arsenic mobility under weakly alkaline and reducing conditions, and furnishes that arsenate reduction by bacteria play a major role leading to high accumulation of desorbed arsenite in groundwater.

© 2018 Elsevier Ltd. All rights reserved.

1. Introduction

Extensive arsenic (As) poisoning events of humans caused by long-term consumption of As-contaminated groundwater have been reported in Bangladesh, and increasing amounts of As contaminated groundwater have been reported worldwide (Smedley and Kinniburgh, 2002; Fendorf et al., 2010; Stuckey et al.,

2016). Accordingly, numerous studies have been conducted to understand the cause of As enrichment in groundwater in different regions, and several mechanisms have been proposed to explain the occurrence of high As groundwater (Chowdhury et al., 1999; Nickson et al., 2000; Islam et al., 2004; Postma et al., 2007; Berg et al., 2008; Xie et al., 2012; Mai et al., 2014; Guo et al., 2016). At present, the prevalent view is that bacterially mediated reductive dissolution of As-bearing Fe (hydr)oxides minerals and subsequent reduction of As results in the release of Fe^{2+} and As(III) into groundwater under reducing conditions (Nickson et al., 2000; Van Geen et al., 2004; Postma et al., 2007; Barringer et al., 2010; Mai

---

et al., 2014). As a result, it is generally believed that high As concentrations occur concurrently with elevated Fe^{2+} concentrations in groundwater. However, this explanation does not hold true for the extremely high As concentrations (maximum $2690\,\mu g\,L^{-1}$) coupled with low Fe^{2+} concentrations in the reducing groundwater of Datong Basin, China.

Under anoxic conditions, bacteria can use As(V), Fe(III) and SO_4^{2-} as an electron acceptor to oxidize organic carbon (or reduced inorganic species), resulting in reduction of these components to As(III), Fe^{2+} and HS^-. Previous studies suggested that these processes are directly related to the fate of As (Oremland and Stolz, 2005; Kirk et al., 2010). For example, Fe (hydr)oxides and clay minerals show stronger adsorption for As(V) than for As(III) at near-neutral pH, therefore, As desorption likely occurred from aquifer sediments when As(V) reduced to As(III) (Martin et al., 2014; Mai et al., 2014). Additionally, reductive dissolution of As-bearing Fe (hydr)oxides minerals can also lead to the release of As from aquifer sediments. Inversely, As can be sequestered by Fe-sulfide minerals (produced by Fe^{2+} and HS^-) through adsorption and/or co-precipitation (Keimowitz et al., 2007; Omoregie et al., 2013; Niazi and Burton, 2016). In addition, sulfide produced by SO_4^{2-} reduction can react with As, resulting in the formation of As-sulfide minerals under relatively high concentrations of As (i.e., μM levels) and HS^- with acidic pH conditions (O'Day et al., 2004; Wilkin and Ford, 2006). Recently, some studies suggest that the dissolved sulfide promotes As mobility via the formation of soluble thioarsenic species at neutral to alkaline environments (Wilkin et al., 2003; Stucker et al., 2014); and can also play significant roles in the abiotic/biotic reduction of Fe(III) (Flynn et al., 2014). All these processes potentially contribute to the release of As into groundwater (Guo et al., 2016). Therefore, the behavior of As depends on As speciation, Fe^{2+}/HS^- concentration, and pH, and could be quite complex and difficult to predict/deduce if As(V), Fe(III) and SO42- reduction processes are occurring (or have previously occurred) in groundwater.

The redox sequence can be a useful means of predicting the approximate order of biogeochemical redox processes from temporal and spatial perspective (Chapelle, 2000). Thus, bacteria are capable of consuming the electron acceptors O_2, NO_3^-, As(V), Fe(III) [$Fe(OH)_3(am)$] and SO_4^{2-} sequentially at pH 7 (Borch et al., 2010). Recently, we investigated the hydrochemical evolution of groundwater along flow path in Datong Basin in an attempt to discriminate As behavior under NO_3^-, As(V), Fe(III) and SO_4^{2-} reduction processes in spatial dimension (Zhang et al., 2017). We revealed that with the exception of a distinct boundary for nitrate reduction process under low As concentration ($<10\,\mu g\,L^{-1}$), no obvious boundaries were observed for other existing hydrochemical processes. Similarly, data generated from a multi-level field pilot study for groundwater As monitoring show that there are elevated concentrations of As(III), Fe^{2+} and HS^- in groundwater in this site (Pi et al., 2016). Interestingly, although Fe^{2+} concentrations ($<0.01-1.17\,mg\,L^{-1}$, average $\sim0.22\,mg\,L^{-1}$, n = 82) (Xie et al., 2013a; Wang et al., 2014; Zhang et al., 2017) in the center part of the basin are elevated compared with those near Piedmont groundwater ($<0.01\,mg\,L^{-1}$) (Zhang et al., 2017), the Fe^{2+} concentrations (in the range of As>$10\,\mu g\,L^{-1}$) are a lot lower than those from other high As groundwater regions, such as Bangladesh ($<0.01-29.2\,mg\,L^{-1}$, average $\sim7.3\,mg\,L^{-1}$, n = 88) (Nickson et al., 2000; Bhattacharya et al., 2009; Halim et al., 2009), Cambodia ($<0.1-26.5\,mg\,L^{-1}$, average $\sim5.2\,mg\,L^{-1}$, n = 40) (Rowland et al., 2008), and Vietnam ($0.4-44.3\,mg\,L^{-1}$, average $13.0\,mg\,L^{-1}$, n = 40) (Berg et al., 2008).

Owing to the seemingly abnormal high As concentrations with relatively low Fe^{2+} concentrations in the groundwater of Datong Basin, further studies are needed to understand the mechanism of As enrichment in groundwater. Thus, this study was designed to further explore the cause(s) of low Fe^{2+} concentrations in the high As groundwater of Datong Basin. More specifically, this study attempt to discriminate the main process [As(V), Fe(III), and SO_4^{2-} reductions] responsible for As mobility, particularly with respect to the behavior of As under SO_4^{2-} reducing conditions. Bacterial community analysis at microcosm and multi-level field monitoring scale were also conducted to better understand the As(V), Fe(III), and SO_4^{2-} reduction processes and dynamics.

2. Materials and methods

2.1. Study site

The study site, Datong Basin, is a Cenozoic Basin located in the semi-arid region of northern China (Wang et al., 2009). The main bedrock is piedmont, with the central basin consisting of the Cenozoic sediments ranging in thickness from 50 to 2500 m (Xie et al., 2009). The organic matter content reaches up to 1% in the aquifer sediments (Wang et al., 2009). From alluvial fans to the central basin (along the groundwater flow path), the groundwater environment evolves from oxidation to reduction conditions and As concentration increased from <1 to $\sim1000\,\mu g\,L^{-1}$ (Zhang et al., 2017). Agricultural activities are usually carried out in the central basin, which suggest a potential source of nitrate addition to the soil through fertilizer application. Evaporites including halite (NaCl), mirabilite ($Na_2SO_4 \cdot 10H_2O$) and gypsum ($CaSO_4 \cdot 2H_2O$) occur as ephemeral accumulations on the land surface, especially in the center of the basin (Xie et al., 2013a). Previously, we suggested that the concentrations of nitrate and sulfate in groundwater will significant affect As behavior and distribution in the study area aquifers as they could be introduced through irrigation and/or precipitation (Xie et al., 2012; Zhang et al., 2017).

A multi-level monitoring network (DY site, Fig. 1) was constructed near the Daying Village, which is located in the central basin. The area of the DY site is $150 \times 250\,m^2$ and groundwater flow direction is approximately from SW to NE (Pi et al., 2016). A total of 32 monitoring wells were installed in three relatively independent semi-confined aquifers (shallow (19–23 m below the land surface), middle (27–29 m) and deep (37–40 m)) for groundwater sampling and monitoring.

2.2. Field samples and analytical methods

Field groundwater and bacteria samples were collected from monitoring wells in August 2013. A total of 32 groundwater samples were extracted from the monitoring wells of the DY site and hydrochemical data and the analytical methods have been described in detail elsewhere (Pi et al., 2016). Eight groundwater bacteria samples were collected from the monitoring wells (B2S, B2M, B2D, C5M, C5D, E1S, E1M and E1D) which represent different burial depth of aquifers. About 10 L of sample water was extracted from monitoring wells, and were filtered through a 0.22-μm cellulose acetate membrane in field laboratory immediately. The membrane filters were subsequently stored in a portable refrigerator at $-20\,°C$ until analysis. DNA extractions were carried out on the membrane filters using PowerWater DNA Isolation Kit (MoBio, Carlsbad, CA 92010, USA). Primer pair 520F (5′-AYTGGGYD-TAAAGNG-3′) and 802R (5′-TACNVGGGTATCTAATCC-3′) were used to amplify bacterial 16S rRNA gene sequences. PCR amplification was implemented in the following steps: initial denaturation at 98 °C for 5 min, followed by 25 cycles of 98 °C for 10 s, 50 °C for 30 s, and 72 °C for 30 s, and then a final extension at 72 °C for 5 min. The purified amplicons were quantified on Microplate reader (BioTek, FLx800) with Quant-iT™ PicoGreen® dsDNA Assay Kit (Invitrogen, P7589) and pooled together. Sample libraries for sequencing were
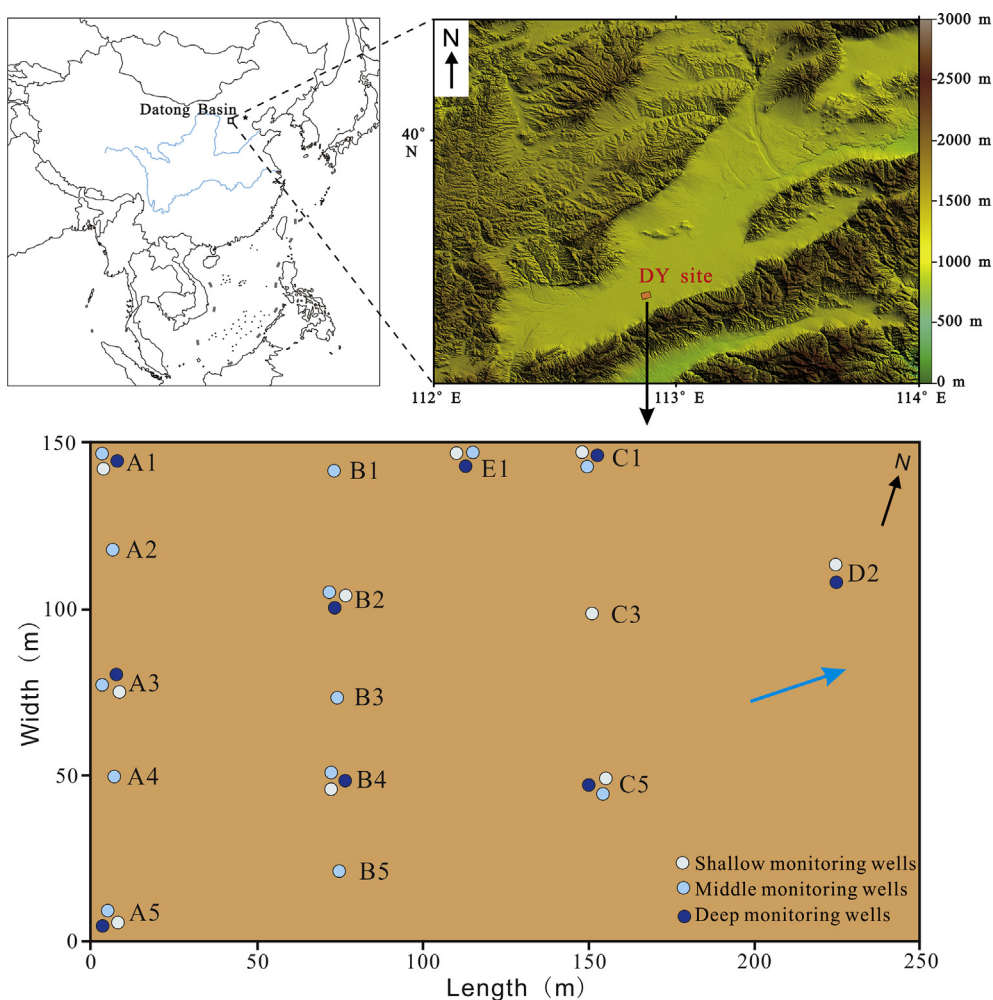
Fig. 1. Diagram of the multi-level monitoring network (DY site) constructed in Datong Basin. The sky blue arrow represents approximate groundwater flow direction in this area. (For interpretation of the references to colour in this figure legend, the reader is referred to the Web version of this article.)

prepared based on published protocols (Jiang et al., 2016). Following, the samples were sequenced on MiSeq Reagent Kit v3 (Illumina, MS-102-3003), then the diversity and relative abundance of prokaryotic communities were analyzed (Degnan and Ochman, 2012).

Sediments were collected for microcosm experiments and other chemical analysis during the well drilling (Fig. S1)**.** Methods for preservation of sediment samples were utilized as reported previously (Pi et al., 2017). Briefly, sediment samples were collected from the core immediately after retrieval by a HDPE liner and then stored in the vacuum bags to eliminate oxygen contact. Thereafter, they were immediately capped into PVC casings, wax-sealed and stored at 4 °C in ice-box. The vacuum bags kept sealed all the time until they were cut off for further experiments in the laboratory.

2.3. Batch microcosm experiments

In order to observe the processes responsible for As mobility, sediments for batch microcosm experiments were selected from low As concentration aquifer (monitoring well B2S, total As$<$10 µg L^{-1}) characterized by brown coarse sand mixed with fine sand and total As and Fe content of about 35 mg kg^{-1} and 24 g kg^{-1}, respectively (Pi et al., 2016), and the total As content is much higher than the average value of 3–10 mg kg^{-1} in modern unconsolidated sediments (Smedley and Kinniburgh, 2013). Our previous studies

suggested that bacterial NO$_3^-$ reduction and SO$_4^{2-}$ reduction processes may have significant impact on As behavior in groundwater (Zhang et al., 2017), therefore, synthetic solution was prepared containing ~1.2 mM nitrate (NaNO$_3$) and 2.3 mM sulfate (K$_2$SO$_4$) as electron acceptors and 12.3 mM acetate (CH$_3$COONa) as electron donor to mimic groundwater solution. All reagents used were guaranteed reagent. The content of acetate was adequate and calculated based on redox reactions to ensure that the added nitrate and sulfate can be fully reduced, including other compounds like readily reducible Fe (hydr)oxides.

About 80 g of uniformly mixed fresh sediments and 250 mL synthetic groundwater were loaded into 75 pre-cleaned and sterilized 300-mL microcosm bottles for water and bacterial communities analysis. Eleven of the 75 bottles were sterilized by autoclaving and used as abiotic controls. To ensure the experiments are initiated in a weakly oxidizing environment (mimicking the groundwater evolution from oxidizing to reducing environment), the oxygen content in each bottle were not completely eliminated during the experimental start-up. The samples were then incubated in a biochemical incubator and placed in the dark, at 30 °C (Guo et al., 2015). To understand the successions of bacterial activities with time, samples were withdrawn from the bottles at intervals until the experiment elapsed. Analytical methods for the water quality parameters have been described previously (Zhang et al., 2017). Briefly, pH and Eh were measured concurrently using

a pre-calibrated multi-parameter portable meter (HACH, HQ40d). Redox active water quality parameters including Fe^{2+}, HS^- and NO_2^- concentrations, were determined immediately using a portable spectrophotometer (HACH, DR2800) after filtering the samples through <0.45 μm cellulose acetate filters. Anions concentrations (NO_3^- and SO_4^{2-}) were determined by ion chromatography (IC) (Metrohm 761 Compact IC). Arsenic concentrations were analyzed using hydride generation atomic fluorescence spectrometry (HG-AFS) (AFS-820, Titan). The average analytical error for anions and As were within 5%.

3. Results

3.1. Hydrochemistry and bacterial community in the multi-level monitoring wells

The maximum and average groundwater As concentration in the multi-level monitoring network site were 2690 μg L^{-1} and 697 μg L^{-1}, respectively. Twenty nine out of 32 samples, contain As exceeding the WHO recommended guideline of 10 μg L^{-1} in drinking water (WHO, 2011), and up to 5 samples were even higher than 1000 μg L^{-1}. The high As groundwater was characterized by weakly alkaline and reducing conditions (pH 7.69 to 8.34, Eh −221.7 to −31.9 mV), with depleted NO_3^- but elevated NH_4^+, and dominated by As(III) species. The Fe^{2+} concentrations (<0.01−0.24 mg L^{-1}, average 0.08 mg L^{-1}) in this site were very low compared with other typical As-contaminated groundwater areas such as Bangladesh (as mentioned above). Additionally, the site was characterized by groundwater with relatively high HS^- concentrations (<1−293 μg L^{-1}; average, 46 μg L^{-1}).

Groundwater bacterial communities were dominated by *Acinetobacter* (5.9−51.3%), *Desulfosporosinus* (4.6−30.2%), *Brevundimonas* (3.9−19%) and *Pseudomonas* (3.2−14.6%) (Fig. 2). In contrast with our previous study results, bacterial communities obtained from oxidizing environment show that *Fluviicola*, *Rhodococcus*, *Glaciecola* and *Nevskia* were identified as the dominant

genera, accounting for 16.89%, 15.46%, 7.21% and 7.23%, respectively (Zhang et al., 2017). *Desulfosporosinus* is a typical sulfate-reducing bacteria (SRB) (Castro et al., 2000), and can also utilize As(V) as an electron acceptor (Oremland and Stolz, 2005). *Acinetobacter*, *Brevundimonas* and *Pseudomonas*, which have also been found to be the main components of bacterial communities in other high As regions (Ghosh and Sar, 2013; Li et al., 2013), generally have higher resistance to As(V) or As(III) (Chitpirom et al., 2009). Furthermore, *Pseudomonas* can reduce As(V) to As(III) by detoxification (Chitpirom et al., 2009) or energy-conserving respiratory pathways (Freikowski et al., 2010). *Flavobacterium*, *Trichococcus*, *Paludibacter* and *Arcobacter* accounted for a relatively high percentage of organisms in several samples (Table S2), but these bacteria have been rarely reported in other areas of high As groundwater. *Geobacter* and *Desulfuromonas*, which belong to the family Geobacteraceae, are typical Fe-reducing bacteria (Fe-RB) that can also use Fe(III)/S^0 as electron acceptors (Lonergan et al., 1996). Moreover, some members of *Geobacter* are capable of dissimilatory reduction of As(V) (Ohtsuka et al., 2013). While the two genera were present in relatively low percentage in most samples, they accounted for 4.6% and 9.3% of the bacteria in sample E1S, respectively.

Hydrochemical results indicated that the high As (mainly As(III)) groundwater in this site is closely associated with a reducing environment, which is in accordance with most of As-contaminated groundwater (Berg et al., 2008; Halim et al., 2009; Guo et al., 2011). However, the groundwater in our study area showed very low Fe^{2+} concentrations with relatively high pH and HS^- concentrations compared with high As groundwater from the Ganges (Nickson et al., 2000; Bhattacharya et al., 2009; Halim et al., 2009) and Mekong (Rowland et al., 2008; Berg et al., 2008) alluvial plain. This, combined with the bacterial information revealed that the dominant genera of the bacterial communities had potential ability to reduce As(V) and SO_4^{2-}, which corresponds to the hydrochemical features of high As(III) and HS^-. Moreover, the low Fe^{2+} concentration appeared to coincide with the low percentage of
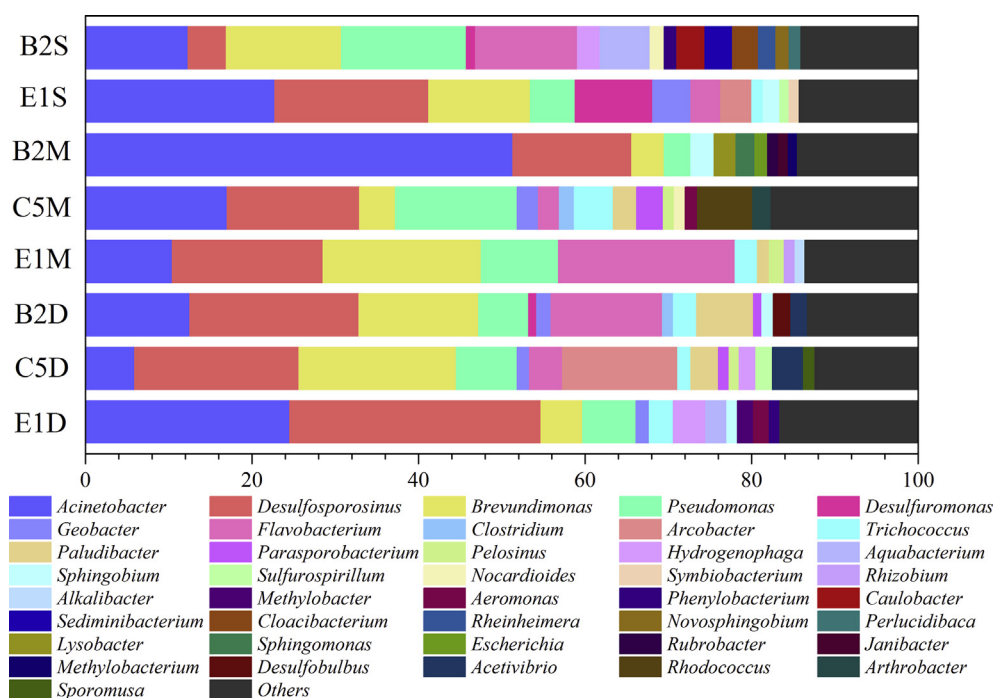

Fig. 2. Bacterial community structure and relatively abundance of bacterial genus based on 16S rRNA clone sequence extracted from field groundwater in DY site. "B2S" (and others) represents the monitoring well ID and the "S", "M" and "D" suffixes represent Shallow, Middle and Deep monitoring wells, respectively.

Fe-RB in most samples, but sample E1S tends to follow a distinct trend with low Fe^{2+}concentration and a high percentage (13.9%) of Fe-RB. Previous studies suggested that As enrichment in groundwater was caused by bacterial mediated As(V) reduction (dissimilatory) (Zobrist et al., 2000; Guo et al., 2015), Fe(III) reduction (Nickson et al., 2000) or SO_4^{2-} reduction process (Stucker et al., 2014). These three mechanisms may all explain the high As groundwater in the study area from the data obtained, but it is unclear which is most significant.

Obviously, high As(III) species found in the groundwater revealed that As(V) have been reduced to As(III) during groundwater evolution. In oxidizing environment, As is generally in the form of As(V) and adsorbed to Fe (hydr)oxides minerals; while reductive dissolution of As-bearing Fe (hydr)oxides will release As(V) and Fe^{2+} into groundwater at reducing conditions. However, previous studies suggested that As(III) is the dominant species in most high As groundwater. Evidences from As biogeochemistry research also confirm this, as many species of bacteria with the ability to reduce As(V) are isolated from As-contaminated regions (Freikowski et al., 2010). The sequencing data obtained from the bacterial community in this study also confirmed the presence of bacterial genera with potential ability to reduce As(V). Generally, As(III) is expected to be less strongly adsorbed than As(V) at near-neutral pH (Smedley and Kinniburgh, 2002; Mai et al., 2014). Thus, bacterially mediated reductive desorption of As(V) may also lead to As(III) enrichment in groundwater (Zobrist et al., 2000; Guo et al., 2015). Therefore, reductive desorption of As(V) contributes to As mobility in the study area groundwater.

The sequential order of Fe(III) and As(V) reduction is a useful information to investigate the mechanism of As mobilization, but this is still under debate. On the basis of the redox sequence (Borch et al., 2010), As(V) reduction occurs before Fe(III) reduction, however, Islam et al. (2004) suggested that As(V) reduction occurs after Fe(III) reduction. Ohtsuka et al. (2013) suggested that As(V) reduced on sediments firstly and then released As(III) into liquid phase during Fe(III) reduction. However, recent studies have shown that bacterial mediated reductive desorption of As(V) is a significant process leading to As(III) mobility in groundwater (Guo et al., 2015; Zhang et al., 2017). Due to the low Fe^{2+} concentrations in high As groundwater of the study area, the following four hypotheses are put forward according to different Fe(III) and As(V) reduction order (Fig. 3).

Briefly, (A) preferential reductive dissolution of As-bearing Fe (hydr)oxides resulting in mobilization of bound As(V) into groundwater and subsequent reduction of As(V) to As(III); (B) preferential reduction of As(V), leading to desorption of As(III) into groundwater and subsequent of release Fe^{2+} through reductive dissolution of Fe(III); (C) initial reduction of As(V) to As(III) on solid phase, followed by Fe(III) reduction resulting in simultaneous release of Fe^{2+} and As(III) into groundwater; (D) reductive desorption of As(V), followed by Fe(III) reduction on solid phase with little release of Fe^{2+} into groundwater.

In the first three cases, the released/dissolved Fe^{2+} probably reacts with CO_3^{2-} or HS^- leading to formation of $FeCO_3$ and Fe-sulfide minerals, with attending decrease in Fe^{2+} concentration. Apparently, while the results are similar, the processes are different (namely, the mechanism of As enrichment in groundwater is different).

Presently, the high As groundwater have undergone long-term evolution, with highly varied hydrochemical components at different stages. Therefore, microcosm incubation experiments may provide important insights into the mechanism of As mobility during the evolution of the high As groundwater.
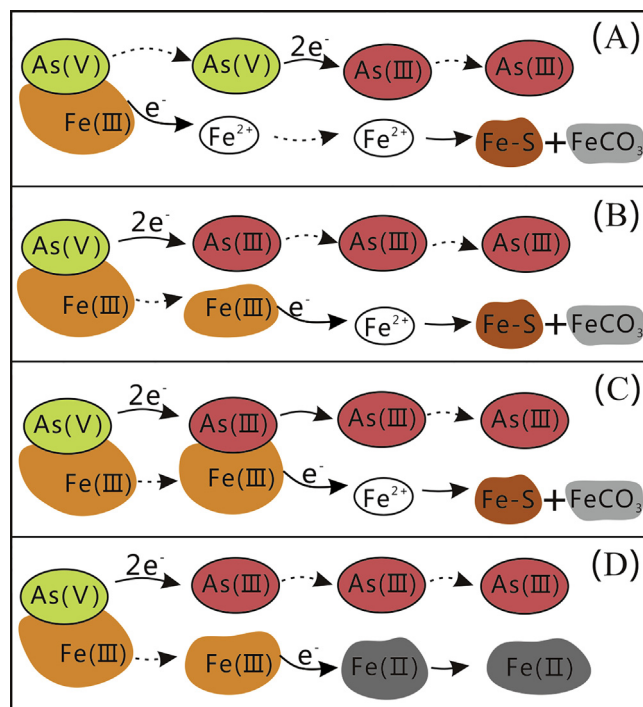

Fig. 3. Suggested hypothesis is governing As mobility in the study area groundwater.

3.2. Microcosm incubation experiments

Laboratory experimental simulations were implemented in an attempt to investigate the reduction mechanism of NO_3^-, As(V), Fe(III) and SO_4^{2-}, and also to discriminate As behavior with incubation time. The chemical compositions of the simulated solutions changed over time (Fig. 4). Notably, the total As concentration increased from ~7 to ~115 $\mu g\ L^{-1}$ during the first 7 d and remained generally stable thereafter. During the first 2 d, NO_3^- decreased gradually, while NO_2^- concentrations initially increased, and then sharply decreased. After 2 d, the concentrations of both NO_3^- and NO_2^- were below detection limits (<0.1 mg L^{-1}) in all the samples. From day 1 to day 7, As(III) concentration gradually increased from <1 to ~100 $\mu g\ L^{-1}$, but the Eh remained relatively stable at ~150 mV Fe^{2+} and HS^- were detected almost simultaneously in solutions on day 5 (Fig. 6) with both gradually and then sharply increasing with time. Fe^{2+} increased up to maximum value of 0.17 mg L^{-1} on day 17, and then decreased afterwards. These chemical components remained relatively stable in sterilized microcosm bottles (Fig. S3). Overall, after 27 d of incubation, the final simulated solutions was weakly alkaline and strongly reducing with high As and HS^- but low Fe^{2+} and depleted NO_3^- (Fig. 4).

Five bacterial samples were obtained from the incubation sediments according to pre-planned experimental timing, and the distribution of the bacterial communities (DOBCs) was analyzed. The DOBC for sample Day 1 differed distinctly from the other four, being dominated by *Pseudomonas* (25%), *Acidovorax* (22.1%), *Acinetobacter* (10.8%), *Lysobacter* (5.9%), *Alishewanella* (5.5%) and *Rheinheimera* (5.6%) (Fig. 5). However, *Pseudomonas*, *Acidovorax* and *Acinetobacter* were present in relatively low percentage in the other four samples (Table S3). The percentage of *Pseudomonas* and *Acinetobacter* gradually decreased with incubation time and had almost disappeared by Day 27. More interestingly, *Symbiobacterium* and *Geobacter* were dominant in the other four samples with percentage of 20—47.2% and 5.5—8.3%, respectively, while they were completely absent on Day 1 (see Fig. 5).
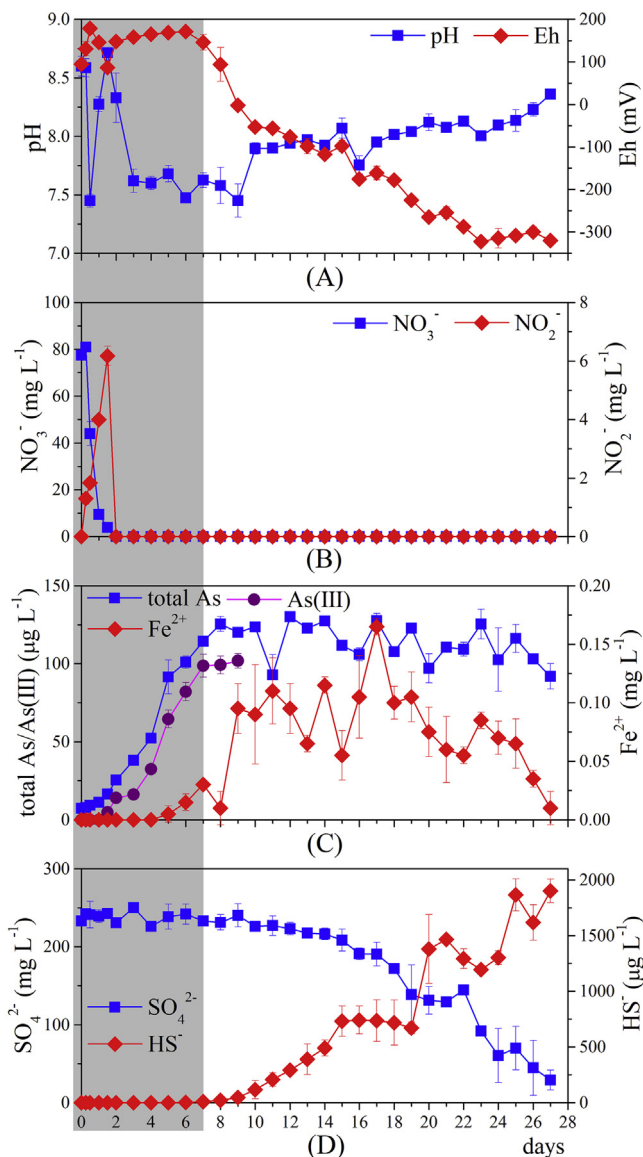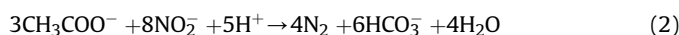
Fig. 4. Hydrochemical components (or parameters) changes with time from microcosm incubation experiments.

The results of the incubation experiments revealed that the chemical compositions of the solutions and sediments' DOBCs evolved concurrently with the incubation time, which is basically consistent with the redox sequence (except for the Fe(III) reduction process) (Borch et al., 2010). At the beginning of the experiment, denitrification represents the main biogeochemical process, which can be inferred by the variation characteristics of NO_3^- and NO_2^- (Eq. (1) and (2)). Additionally, genus *Acidovorax* (22.1%) which account for a high percentage in sample Day 1 has potential abilities to reduce NO_3^- (Heylen et al., 2008).

$$CH_3COO^- + 4NO_3^- \rightarrow 4NO_2^- + 2HCO_3^- + H^+ \quad (1)$$

$$3CH_3COO^- + 8NO_2^- + 5H^+ \rightarrow 4N_2 + 6HCO_3^- + 4H_2O \quad (2)$$

When NO_3^- is almost depleted, the As(V) reduction process begins, resulting in the gradual increase of As(III) concentration until it reaches ~100 μg L^{-1} (Fig. 6A). Obviously, the process by which bacteria reduced As(V) to As(III) led to desorption of As from

sediments and became enriched in the solutions. Unexpectedly, Fe(III) reduction was initiated while As(V) reduction was still occurring. In addition, Fe(III) and SO_4^{2-} reduction showed no obvious margins but started almost simultaneously (Fig. 6B). Although SO_4^{2-} reduction occurred distinctly according to variations in SO_4^{2-} and HS^- concentrations, almost no SRB was observed in the samples (see Section 4).

4. Discussion

4.1. Low Fe^{2+} concentrations in high As groundwater

Extremely low Fe^{2+} concentrations (<0.01–0.24 mg L^{-1}, average 0.08 mg L^{-1}) was observed in the multi-level monitoring network site groundwater, with characteristically high As concentration (generally >500 μg L^{-1}), which was also found throughout the Datong Basin (Xie et al., 2013a). Similarly, some high As groundwater from other areas have reportedly showed very low concentration of Fe^{2+} and are characterized by weakly alkaline and reducing conditions (Welch and Lico, 1998; Lu et al., 2011; Zhou et al., 2017). Additionally, high As groundwater with low Fe^{2+} concentrations in oxidizing conditions have been reported recently (Shakoor et al., 2015; Podgorski et al., 2017). Following the results shown in our previous studies (Pi et al., 2016; Zhang et al., 2017) where we described the saturation indices of FeS and FeCO₃, it is clear that precipitation of these minerals is not the main reason for the low Fe^{2+} concentrations in groundwater hence, we propose two possible processes explaining the reason for the low Fe^{2+} concentration throughout the high As groundwater evolution. First, is the relatively retarded Fe(III) reduction process due to high pH conditions. Secondly, partial Fe(III) reduction to Fe(II) on solid phase at the initiation of SO_4^{2-} reduction process. Therefore, most Fe(II) was not released into groundwater, but was instead transformed to other Fe minerals in-situ (such as mackinawite or magnetite) (Xie et al., 2009; Kocar et al., 2010; Pi et al., 2017).

Bacterially mediated Fe(III) reduction processes are severely inhibited when pH increases from 6.8 to 9 (Flynn et al., 2014). This is mainly due to the reduction of Fe (hydr)oxides minerals, which will consume several protons (H$^+$) (Eq. (3)); therefore, the reaction is gradually retarded as the pH increases.

$$CH_3COO^- + 8Fe(OH)_3 + 15H^+ \rightarrow 8Fe^{2+} + 20H_2O + 2HCO_3^- \quad (3)$$
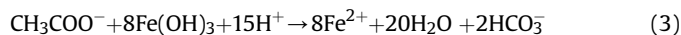
As a result, SO_4^{2-} reduction will exclude Fe(III) reduction in alkaline groundwater because it yields more energy than Fe(III) reduction (Bethke et al., 2011). To further explore the relationship between Fe^{2+} and pH, we collected the data describing Fe^{2+} concentrations and pH from several high As groundwater regions and selected data for which the total As concentrations were higher than 10 μg L^{-1} and then evaluated the relationship between Fe^{2+} and pH. The results show that Fe^{2+} is negatively correlated with pH (Fig. 7), which is consistent with the view that Fe(III) reduction relative to SO_4^{2-} reduction tends to increase with decreasing pH (Kirk et al., 2016). Moreover, the Fe^{2+} concentrations decrease dramatically when the pH is higher than 7.5. Similarly, there is a significant negative correlation between Fe^{2+} and pH in Datong Basin, but no obvious correlation between Fe^{2+} and total As (Fig. S4).

Although direct reduction of Fe(III) by bacteria is initially inhibited under alkaline conditions, bacteria can reduce Fe(III) indirectly by using S^0 (electron shuttling) or HS$^-$ to reduce Fe(III) abiotically when SO_4^{2-} reduction is occurring (Flynn et al., 2014). As a result, the relationship between Fe-RB and SRB is more likely due to mutualism rather than competition (Bethke et al., 2011). The results of the incubation experiments also showed that Fe^{2+} and
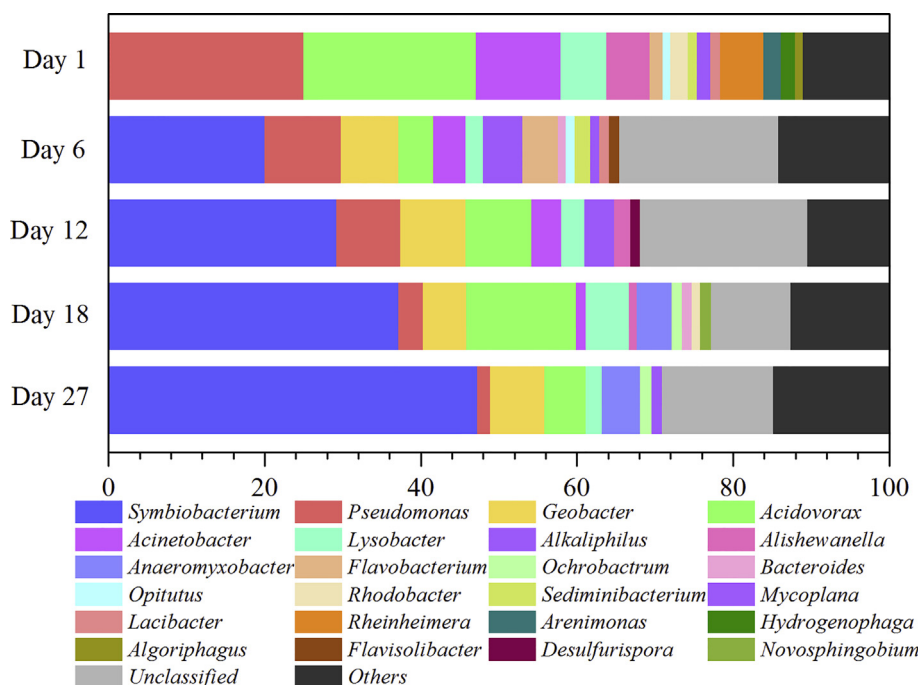
Fig. 5. Bacterial community structure and relatively abundance of bacterial genus based on 16S rRNA clone sequence extracted from sediments of microcosm incubation experiments.
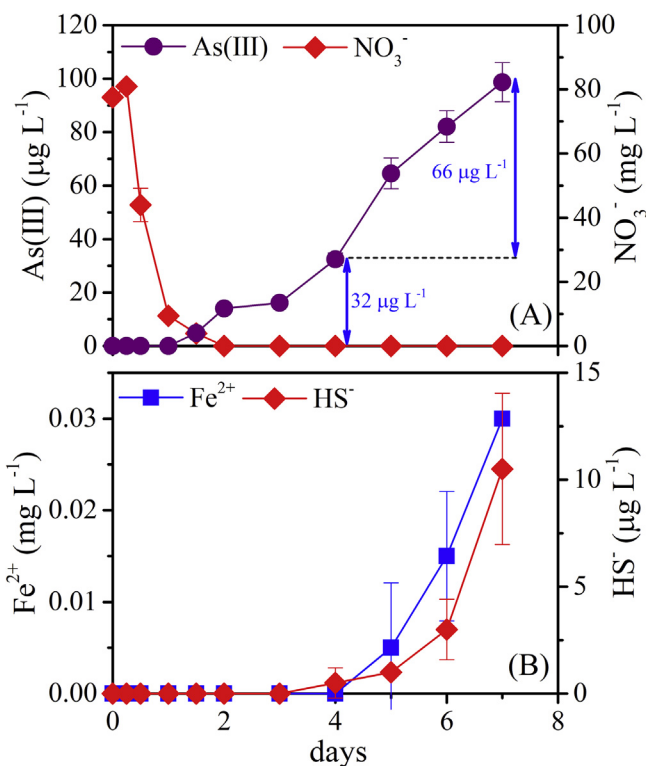

Fig. 6. Part of hydrochemical components changes with time (day 1 to day 7) from microcosm incubation experiments.

HS$^-$ were detected in solutions almost simultaneously on day 5 (Fig. 6B). The following three equations explain the process clearly. Among these equations, Eqs. (4) and (7) is mediated by bacteria and Eqs. (5) and (6) are abiotic.
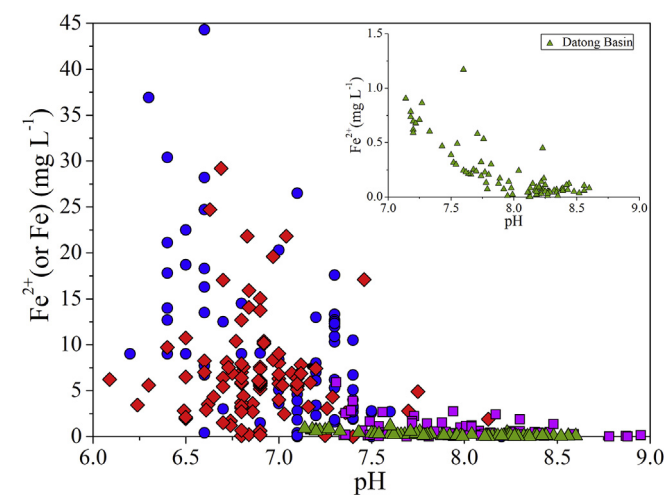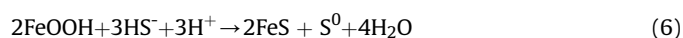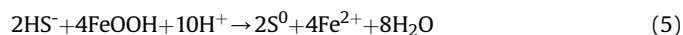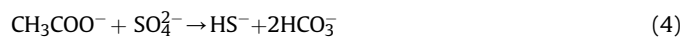

Fig. 7. Relationship between Fe^{2+} (or dissolved Fe) concentrations and pH in high As groundwater (As>10 μg L^{-1}) from different countries or regions. Blue circles represent Cambodia and Vietnam (data from Rowland et al., 2008; Berg et al., 2008), red diamonds represent Bangladesh and West Bengal (India) (data from Nickson et al., 2000; Bhattacharya et al., 2009; Halim et al., 2009; Stüben et al., 2003), purple squares represent Inner Mongolia (China) (data from Guo et al., 2008, 2011), and olive triangle represent Datong (China) (data from Zhang et al., 2017; Xie et al., 2013a; Wang et al., 2014; and fraction of data from this survey). (For interpretation of the references to colour in this figure legend, the reader is referred to the Web version of this article.)

$$CH_3COO^- + SO_4^{2-} \rightarrow HS^- + 2HCO_3^- \qquad (4)$$

$$2HS^- + 4FeOOH + 10H^+ \rightarrow 2S^0 + 4Fe^{2+} + 8H_2O \qquad (5)$$

$$2FeOOH + 3HS^- + 3H^+ \rightarrow 2FeS + S^0 + 4H_2O \qquad (6)$$

$$CH_3COO^- + 4S^0 + 4H_2O \rightarrow 4HS^- + 2HCO_3^- + 5H^+ \qquad (7)$$

S^0 can be substituted as the electron acceptor for genus

Geobacter (Lonergan et al., 1996), after which, S^0 is reduced reversibly to HS^-. Meanwhile, Fe^{2+} cannot accumulate to a high concentration in solutions under strongly SO_4^{2-} reducing conditions because a fraction of them can be precipitated with HS^- to form mackinawite (FeS) (Burton et al., 2014). In the incubation experiments, Fe^{2+} concentrations show a decreasing tendency with increasing concentrations of HS^- from day 17 to day 27, likely due to formation of Fe-sulfide minerals. However, this scenario may not correspond to the field groundwater because the HS^- concentrations were not so high. Furthermore, the saturation indices of mackinawite in groundwater also confirm that most groundwater with low Fe^{2+} concentrations cannot simply be explained by precipitation of Fe-sulfide minerals. Probably, most of Fe(III) is chemically reduced to Fe(II) by HS^- in-situ and transformed to other forms of Fe minerals (Kocar et al., 2010), thereby preventing the release of large amounts of Fe^{2+} into groundwater, as described in Eq. (6). Recent study of sediments in this site also suggest that Fe(II) accounted for a large part of the crystalline Fe (15.17%–30.81%) (Pi et al., 2016). On the other hand, the incubation experiments show that the SO_4^{2-} concentrations were decreased by about 200 mg L^{-1} (from 230 to 30 mg L^{-1}) through 27 d incubation, however, HS^- concentrations only increased to about 2 mg L^{-1} in the residual solution. Owing to the fact that the microcosm bottle is a closed system, which suggests that most of the produced HS^- are embedded in the sediments on the basis of conservation of matter, although a small portion of H_2S will be present in the headspace of the bottle.

Generally, the dominant genera of the bacterial communities corresponding to main biogeochemical process, like the SRB have high percentage ratios in field groundwater due to strong SO_4^{2-} reduction process there. However, the bacterial samples obtained from groundwater (liquid phase) and sediments (solid phase) in the same environment condition may have variable dominant genera in the two phases. As discussed previously, the Fe-RB and SRB are involved in a mutualistic relationship; however, the Fe-RB (genus *Geobacter*) accounted for relatively high percentage (5.5–8.3%) in the experimental sediments samples (except for sample Day 1), while SRB was almost completely absent from these samples. Conversely, SRB was found to comprise 4.6–30.2% of field groundwater sample populations, but the Fe-RB percentage were very low (<2.6%) (except for sample E1S). Although, these results seem to contradict the view that these two types of reducing bacteria have a mutualistic relationship, these findings are not inconsistent, but rather simply reflect variations based on the type of electron acceptor they are using. SO_4^{2-} is dissolved in solution (or groundwater), but Fe(III) is an insoluble solid in sediments. As a result, Fe-RB will be mainly attached to sediment, while SRB were suspended in solution (or groundwater). Flynn et al. (2013) also found that Fe-RB (*Geobacter* sp.) were present in greater abundance in sediments than groundwater. Field groundwater sample E1S had a relatively high percentage of genus *Geobacter*, this is probably due to sediment influx (relatively turbid water was observed) during the extraction of the groundwater. This may be the main reason for SRB almost complete absence from experimental sediments, although strong SO_4^{2-} reduction occurred. Unfortunately, analysis of the bacterial communities in the experimental liquid phase was not quantified due to insufficient solutions for enriching bacterial samples and hence, requires further investigation.

4.2. The mechanism of arsenic enrichment in groundwater

According to previous studies, bacterially mediated Fe(III), SO_4^{2-} and As(V) reduction have all contributed to As mobility in the study area (Xie et al., 2013a; Pi et al., 2017; Zhang et al., 2017). However, these three mechanisms, as important as they are, remain largely unclear.

Apparently, reductive dissolution of Fe (hydr)oxide minerals may have contributed to As mobility in the study area groundwater, but the possibility remain very low. Sediments analysis in the site suggested that Fe-bearing minerals function as important sinks for As in aquifers. Moreover, readily reducible Fe content (normally in amorphous or poorly crystalline form) ranged from 3.71 to 10.27 g kg^{-1} (mean: 5.66 g kg^{-1}), and As content in the readily reducible Fe phase ranged from 1.37 to 38.25 mg kg^{-1} (mean: 5.58 mg kg^{-1}) with most existing as As(V) (Pi et al., 2016). Thus, ratios of As/Fe can be roughly estimated at 1:1000 (maximum ~1:100) in sediments. Assuming that reductive dissolution of As-bearing Fe (hydr)oxide minerals occurred and Fe^{2+} and As are all released into groundwater simultaneously, the results would be that Fe^{2+} concentrations will be 1000 times higher (at least ~100 times) than As concentrations and As(V) will be the dominant As species in the groundwater. However, data from field groundwater does not match this speculation, but instead the opposite, where As (mainly As(III)) concentrations is several tens of times and even more higher than Fe^{2+}. It is also contradictory to explain that the low Fe^{2+} concentrations occurred due to re-precipitation (Section 4.1). Results from incubation experiments suggest that As enrichment in solutions is likely decoupled from Fe(III) reduction. This is because, As concentrations in solutions increased from 7 to ~52 μg L^{-1} with incubation time from day 1 to day 4, however, Fe^{2+} remains below the detection limit of 0.01 mg L^{-1}. From day 5 to day 7, although As concentrations increased with increasing Fe^{2+}, As(III) and Fe^{2+} concentrations increased only by ~62 μg L^{-1} and 30 μg L^{-1} (ratio of As/Fe^{2+} = ~2), respectively. Furthermore, Fe^{2+} only shows gradual increase and thus, excludes re-precipitation process as the main reason for low Fe^{2+} during day 5 to day 7.

Under SO_4^{2-} reducing conditions, the transformation between crystalline Fe(III) and poorly crystalline Fe phase could result in repartition of As in the solid phase and release partial As into liquid phase (Kocar et al., 2010; Xie et al., 2013b). It is worth to note that the net increase in concentration of As(III) in the experiment from day 2 to day 4 and day 5 to day 7 is 32 μg L^{-1} and 66 μg L^{-1}, respectively (Fig. 6A). Obviously, As(III) concentration increased more rapidly when SO_4^{2-} reduction was initiated. This may be due to crystalline Fe(III) reduction by HS^- abiotically (as described Eq. (6)) at that instance, and the formation of FeS (mackinawite) minerals which have relatively low ability to absorb As(III) (Kocar et al., 2010; Burton et al., 2011). Field study report also suggested that transformation of Fe (hydr)xoides to mackinawite could increase As mobility at the Datong aquifers (Pi et al., 2017). On the other hand, SO_4^{2-} reduction process may promote As mobility due to formation of thioarsenic species which has weakly adsorption properties and high solubility (Bostick et al., 2005; Burton et al., 2013). However, thioarsenic is unlikely to be the main form of As in groundwater due to the relatively low HS^-. Previous studies suggested that thioarsenites dominate As speciation at sulfide concentrations >$10^{-4.3}$ M (~1.6 mg L^{-1}) and at neutral pH (Wilkin et al., 2003). However, the average HS^- is only 46 μg L^{-1} (maximum is 293 μg L^{-1}) in the groundwater. Results from incubation experiments suggest that HS^- concentrations increased strongly after 8 d and reached a maximum of ~2000 μg L^{-1}. However, total As concentration stabilized at around 120 μg L^{-1} during this period. Therefore, the high HS^- neither obviously promoted As released, nor significantly decreased the total As content in the solutions. As(III) may be partially transformed to thioarsenites due to the high HS^- concentration in solutions (Eq. (8) (Wilkin et al., 2003)).
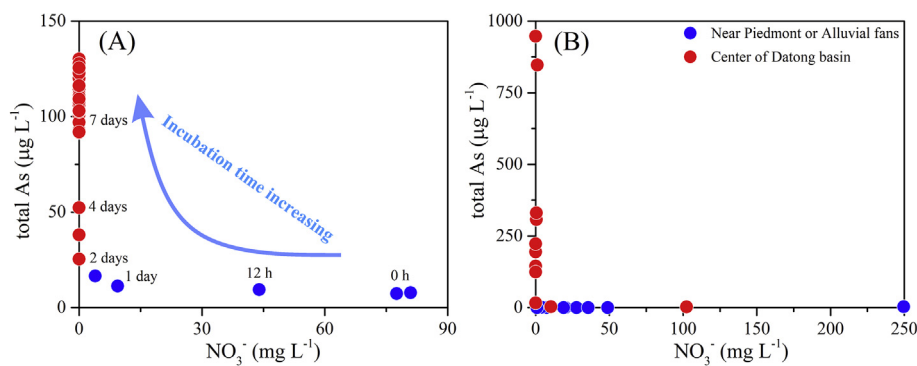
$$H_3AsO_3 + HS^- \rightleftharpoons H_2AsO_2S^- + H_2O \qquad (8)$$
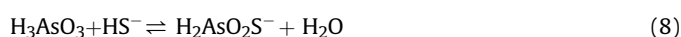
Fig. 8. Relationships between total As and NO_3^- concentration in incubation experiment solutions (A) and field groundwater (B. is adopted from Zhang et al., 2017).

Thus, it is more likely that the dissolved As(III) transform to thioarsenites, which is an important process in high HS^- solutions or groundwater, but arguably not the main mechanism for As mobility in the study area.

Bacterially mediated reductive desorption of As(V) may be the main reason for As mobility in this groundwater site. According to our previous study, the occurrence of high As groundwater in this area followed a gradual evolution process along the groundwater flow path (Zhang et al., 2017), and shows agreement with the microcosm experiments described in section 3.2. Accordingly, the occurrence of high As groundwater in the study site should be considered a long-term evolution that has led to Fe(III) and SO_4^{2-} reduction, which is also currently occurring in the site. In addition, the field conditions were similar in chemistry to the synthetic solutions at around Day 10 of the experiment, accompanying low Fe^{2+} (~0.1 mg L^{-1}) that coexisted with elevated HS^- (~116 μg L^{-1}) at weakly alkaline (pH 7.9) and reducing conditions (Eh −53 mV). Therefore, As(V) reduction process has obviously occurred, leading to As(III) desorption and elevated total As concentrations in natural groundwater. Results from sediments analysis indicate that As species occurred in easily reducible Fe phase (normally in amorphous or poorly crystalline form) and mostly existed as As(V) (Pi et al., 2016). Moreover, clay minerals also have preferential adsorption for As(V) (Goldberg, 2002). Similarly, bacteria reduction of As(V) to As(III) generated As species that desorbed from sediments due to the relatively weak adsorption of As(III). This speculation is consistent with the field groundwater condition, which show that As(III) is the dominant total As species. In addition, results from the microcosm experiment also indicate that total As in solutions increased with increase in As(III). On the other hand, we found that the relationship between total As and NO_3^- were in accordance with the field survey results obtained from the Datong basin previously, which reflect that As reduction is inhibited by NO_3^- reduction (Fig. 8). Similarly, these findings are consistence with the redox sequence for As(V) reduction occurring after NO_3^- reduction. Therefore, we put forward that reductive desorption of As(V) is the main process controlling As mobility in this region.

5. Conclusion

Previous studies have shown that bacterially mediated reductive dissolution of As-bearing Fe (hydr)oxide minerals is the main process for As enrichment in anoxic groundwater. However, this process does not explain the very low Fe^{2+} concentrations with extremely high As in groundwater of Datong Basin. The groundwater was characterized by high HS^- and pH, and as a result, the bacteria mediated Fe(III) reduction process is probably inhibited by high pH initially and, the SO_4^{2-} reduction process occurring in the groundwater. Results from our microcosm experiment confirmed this. Furthermore, under a SO_4^{2-} reducing environment, Fe(III) is chemically reduced by HS^- (or bacteria reduces Fe(III) indirectly) and a part of As released. Nevertheless, Fe^{2+} cannot accumulate to a high concentration because it can be reduced in-situ and immobilized by HS^- to form Fe-sulfide minerals. More interestingly, the bacterial As(V) reduction process proceeded before Fe(III) (bacterial or chemical) and SO_4^{2-} reduction in the incubation experiment, and the total As concentration (dominated by As(III)) gradually increased as As(V) was reduced. Based on these findings, we conclude that the bacterially mediated reductive desorption of As(V) is the major process leading to As enrichment in the weakly alkaline and reducing groundwater of Datong Basin.

Acknowledgements

Appendix A. Supplementary data

Supplementary data related to this article can be found at https://doi.org/10.1016/j.envpol.2018.01.092.

References

Barringer, J.L., Mumford, A., Young, L.Y., Reilly, P.A., Bonin, J.L., Rosman, R., 2010. Pathways for arsenic from sediments to groundwater to streams: biogeochemical processes in the Inner Coastal Plain, New Jersey, USA. Water Res. 44, 5532–5544.

Berg, M., Trang, P.T.K., Stengel, C., Buschmann, J., Viet, P.H., Dan, N.V., Giger, W., Stüben, D., 2008. Hydrological and sedimentary controls leading to arsenic contamination of groundwater in the Hanoi area, Vietnam: the impact of iron-arsenic ratios, peat, river bank deposits, and excessive groundwater abstraction. Chem. Geol. 249, 91–112.

Bethke, C.M., Sanford, R.A., Kirk, M.F., Jin, Q., Flynn, T.M., 2011. The thermodynamic ladder in geomicrobiology. Am. J. Sci. 311, 183–210.

Bhattacharya, P., Hasan, M.A., Sracek, O., Smith, E., Ahmed, K.M., Brömssen, M., Huq, S.M.I., Naidu, R., 2009. Groundwater chemistry and arsenic mobilization in the Holocene flood plains in south-central Bangladesh. Environ. Geochem. Health 31, 23–43.

Borch, T., Kretzschmar, R., Kappler, A., Cappellen, P.V., Ginder-Vogel, M., Voegelin, A., Campbell, K., 2010. Biogeochemical redox processes and their impact on contaminant dynamics. Environ. Sci. Technol. 44, 15–23.

Bostick, B.C., Fendorf, S., Brown, G.E., 2005. In situ analysis of thioarsenite complexes in neutral to alkaline arsenic sulphide solutions. Mineral. Mag. 69, 781–795.

Burton, E.D., Johnston, S.G., Bush, R.T., 2011. Microbial sulfidogenesis in ferrihydrite-rich environments: effects on iron mineralogy and arsenic mobility. Geochem. Cosmochim. Acta 75, 3072–3087.

Burton, E.D., Johnston, S.G., Planer-Friedrich, B., 2013. Coupling of arsenic mobility to sulfur transformations during microbial sulfate reduction in the presence

and absence of humic acid. Chem. Geol. 343, 12—24.

Burton, E.D., Johnston, S.G., Kocar, B.D., 2014. Arsenic mobility during flooding of contaminated soil: the effect of microbial sulfate reduction. Environ. Sci. Technol. 48 (23), 13660—13667.

Castro, H.F., Williams, N.H., Ogram, A., 2000. Phylogeny of sulfate-reducing bacteria. FEMS Microbiol. Ecol. 31, 1—9.

Chapelle, F.H., 2000. The significance of microbial processes in hydrogeology and geochemistry. Hydrogeol. J. 8, 41—46.

Chowdhury, T.R., Basu, G.K., Mandal, B.K., Biswas, B.K., Samanta, G., Chowdhury, U.K., Chanda, C.R., Lodh, D., Roy, S.L., Saha, K.C., 1999. Arsenic poisoning in the Ganges delta. Nature 401, 545—546.

Chitpirom, K., Akaracharanya, A., Tanasupawat, S., Leepipatpibooim, N., Kyoungwoong, K., 2009. Isolation and characterization of arsenic resistant bacteria from tannery wastes and agricultural soils in Thailand. Ann. Microbial 59, 649—656.

Degnan, P.H., Ochman, H., 2012. Illumina-based analysis of microbial community diversity. ISME J. 6, 183—194.

Fendorf, S., Michael, H.A., Geen, A.V., 2010. Spatial and temporal variations of groundwater arsenic in south and southeast Asia. Science 328, 1123—1127.

Flynn, T.M., Sanford, R.A., Ryu, H., Bethke, C.M., Levine, A.D., Ashbolt, N.J., Santo Domingo, J.W., 2013. Functional microbial diversity explains groundwater chemistry in a pristine aquifer. BMC Microbial 13, 146.

Flynn, T.M., O'Loughlin, E.J., Mishra, B., DiChristina, T.J., Kemner, K.M., 2014. Sulfur-mediated electron shuttling during bacterial iron reduction. Science 344, 1039—1042.

Freikowski, D., Winter, J., Gallert, C., 2010. Hydrogen formation by an arsenate-reducing Pseudomonas putida, isolated from arsenic-contaminated ground-water in West Bengal, India. Appl. Microbiol. Biotechnol. 88, 1363—1371.

Ghosh, S., Sar, P., 2013. Identification and characterization of metabolic properties of bacterial populations recovered from arsenic contaminated ground water of North East India (Assam). Water Res. 47, 6992—7005.

Goldberg, S., 2002. Competitive adsorption of arsenate and arsenite on oxides and clay minerals. Soil Sci. Soc. Am. J. 66 (2), 413—421.

Guo, H., Yang, S., Tang, X., Li, Y., Shen, Z., 2008. Groundwater geochemistry and its implications for arsenic mobilization in shallow aquifers of the Hetao Basin. Inner Mongolia. Sci. Total Envion 393, 131—144.

Guo, H., Zhang, B., Li, Y., Berner, Z., Tang, X., Norra, S., Stüben, D., 2011. Hydro-geological and biogeochemical constrains of arsenic mobilization in shallow aquifers from the Hetao basin, Inner Mongolia. Environ. Pollut. 159, 876—883.

Guo, H., Liu, Z., Ding, S., Hao, C., Xiu, W., Hou, W., 2015. Arsenate reduction and mobilization in the presence of indigenous aerobic bacteria obtained from high arsenic aquifers of the Hetao basin, Inner Mongolia. Environ. Pollut. 203, 50—59.

Guo, H., Zhou, Y., Jia, Y., Tang, X., Li, X., Shen, M., Han, S., Wei, C., Norra, S., Zhang, F., 2016. Sulfur cycling-related biogeochemical processes of arsenic mobilization in the western hetao basin, China: evidence from multiple isotope Approaches. Environ. Sci. Technol. 50, 12650—12659.

Halim, M.A., Majumder, R.K., Nessa, S.A., Hiroshiro, Y., Uddin, M.J., Shimada, J., Jinno, K., 2009. Hydrogeochemistry and arsenic contamination of groundwater in the Ganges delta plain, Bangladesh. J. Hazard. Mater 164, 1335—1345.

Heylen, K., Lebbe, L., Vos, P.D., 2008. Acidovorax caeni sp. nov., a denitrifying species with genetically diverse isolates from activated sludge. Int. J. Syst. Evol. Microbiol. 58, 73—77.

Islam, F.S., Gault, A.G., Boothman, C., Polya, D.A., Charnock, J.M., Chatterjee, D., Lloyd, J.R., 2004. Role of metal-reducing bacteria in arsenic release from Bengal delta sediments. Nature 430, 68—71.

Jiang, Z., Li, P., Van Nostrand, J.D., Zhang, P., Zhou, J., Wang, Y., Dai, X., Zhang, R., Jiang, D., Wang, Y., 2016. Microbial communities and arsenic biogeochemistry at the outflow of an alkaline sulfide-rich hot spring. Sci. Rep. 6.

Keimowitz, A.R., Mailloux, B.J., Cole, P., Stute, M., Simpson, H.J., Chillrud, S.N., 2007. Laboratory investigations of enhanced sulfate reduction as a groundwater arsenic remediation strategy. Environ. Sci. Technol. 41, 6718—6724.

Kirk, M.F., Roden, E.E., Crossey, L.J., Brealey, A.J., Spilde, M.N., 2010. Experimental analysis of arsenic precipitation during microbial sulfate and iron reduction in model aquifer sediment reactors. Geochem. Cosmochim. Acta 74, 2538—2555.

Kirk, M.F., Jin, Q., Haller, B.R., 2016. Broad-scale evidence that pH influences the balance between microbial iron and sulfate reduction. Ground Water 54, 406—413.

Kocar, B.D., Borch, T., Fendorf, S., 2010. Arsenic repartitioning during biogenic sul-fidization and transformation of ferrihydrite. Geochem. Cosmochim. Acta 74, 980—994.

Li, P., Wang, Y., Jiang, Z., Jiang, H., Li, B., Dong, H., Wang, Y., 2013. Microbial diversity in high arsenic groundwater in hetao basin of inner Mongolia, China. Geo-microbiol. J. 30, 897—909.

Lonergan, D.J., Jenter, H.L., Coates, J.D., Phillips, E.J., Schmidt, T.M., Lovley, D.R., 1996. Phylogenetic analysis of dissimilatory Fe(III)-reducing bacteria. J. Bacteriol. 178, 2402—2408.

Lu, K.L., Liu, C.W., Wang, S.W., Jang, C.S., Lin, K.H., Liao, V.H.C., Liao, C.M., Chang, F.J., 2011. Assessing the characteristics of groundwater quality of arsenic contami-nated aquifers in the Blackfoot disease endemic area. J. Hazard Mater. 185 (2), 1458—1466.

Mai, N.T.H., Postma, D., Trang, P.T.K., Jessen, S., Viet, P.H., Larsen, F., 2014. Adsorption and desorption of arsenic to aquifer sediment on the Red River floodplain at Nam Du. Vietnam. Geochim. Cosmochim. Acta 142, 587—600.

Martin, M., Violante, A., Ajmone-Marsan, F., Barberis, E., 2014. Surface interactions of arsenite and arsenate on soil colloids. Soil Sci. Soc. Am. J. 78 (1), 157—170.

Niazi, N.K., Burton, E.D., 2016. Arsenic sorption to nanoparticulate mackinawite (FeS): an examination of phosphate competition. Environ. Pollut. 218, 111—117.

Nickson, R.T., Mcarthur, J.M., Ravenscroft, P., Burgess, W.G., Ahmed, K.M., 2000. Mechanism of arsenic release to groundwater, Bangladesh and West Bengal. Appl. Geochem. 15, 403—413.

Ohtsuka, T., Yamaguchi, N., Makino, T., Sakurai, K., Kimura, K., Kudo, K., Homma, E., Dong, D.T., Amachi, S., 2013. Arsenic dissolution from Japanese paddy soil by a dissimilatory arsenate-reducing bacterium Geobacter sp. OR-1. Environ. Sci. Technol. 47, 6263—6271.

Omoregie, E.O., Couture, R.M., Van, C.P., Corkhill, C.L., Charnock, J.M., Polya, D.A., Vaughan, D., Vanbroekhoven, K., Lloyd, J.R., 2013. Arsenic bioremediation by biogenic iron oxides and sulfides. Appl. Environ. Microbiol. 79, 4325—4335.

Oremland, R.S., Stolz, J.F., 2005. Arsenic, microbes and contaminated aquifers. Trends Microbiol. 13, 45—49.

O'Day, P.A., Vlassopoulos, D., Root, R., Rivera, N., 2004. The influence of sulfur and iron on dissolved arsenic concentrations in the shallow subsurface under changing redox conditions. Proc. Natl. Acad. Sci. U. S. A 101, 13703—13708.

Postma, D., Larsen, F., Hue, N.T.M., Mai, T.D., Viet, P.H., Nhan, P.Q., Jessen, S., 2007. Arsenic in groundwater of the Red River floodplain, Vietnam: controlling geochemical processes and reactive transport modeling. Geochem. Cosmochim. Acta 71, 5054—5071.

Podgorski, J.E., Eqani, S.A.M.A.S., Khanam, T., Ullah, R., Shen, H., Berg, M., 2017. Extensive arsenic contamination in high-pH unconfined aquifers in the Indus Valley. Sci. adv 3 (8) e1700935.

Pi, K., Wang, Y., Xie, X., Liu, Y., Ma, T., Su, C., 2016. Multilevel hydrogeochemical monitoring of spatial distribution of arsenic: a case study at Datong Basin, northern China. J. Geochem. Explor. 161, 16—26.

Pi, K., Wang, Y., Xie, X., Ma, T., Su, C., Liu, Y., 2017. Role of sulfur redox cycling on arsenic mobilization in aquifers of Datong Basin, northern China. Appl. Geo-chem. 77, 31—43.

Rowland, H.A., Gault, A.G., Lythgoe, P., Polya, D.A., 2008. Geochemistry of aquifer sediments and arsenic-rich groundwaters from Kandal Province, Cambodia. Appl. Geochem. 23, 3029—3046.

Shakoor, M.B., Niazi, N.K., Bibi, I., Rahman, M.M., Naidu, R., Dong, Z., Shahid, M., Arshad, M., 2015. Unraveling health risk and speciation of arsenic from groundwater in rural areas of Punjab, Pakistan. Int. J. Environ. Res. Publ. Health 12 (10), 12371—12390.

Smedley, P.L., Kinniburgh, D.G., 2002. A review of the source, behaviour and dis-tribution of arsenic in natural waters. Appl. Geochem. 17, 517—568.

Smedley, P.L., Kinniburgh, D.G., 2013. Arsenic in groundwater and the environment. In: Essentials of Medical Geology. Springer Netherlands, pp. 279—310.

Stuckey, J.W., Sparks, D.L., Fendorf, S., 2016. Delineating the convergence of biogeochemical factors responsible for arsenic release to groundwater in south and southeast Asia. Adv. Agron. 140, 43—74.

Stucker, V.K., Silverman, D.R., Williams, K.H., Sharp, J.O., Ranville, J.F., 2014. Thio-arsenic species associated with increased arsenic release during biostimulated subsurface sulfate reduction. Environ. Sci. Technol. 48, 13367—13375.

Stüben, D., Berner, Z., Chandrasekharam, D., Karmakar, J., 2003. Arsenic enrichment in groundwater of West Bengal, India: geochemical evidence for mobilization of as under reducing conditions. Appl. Geochem. 18, 1417—1434.

Van Geen, A., Rose, J., Thoral, S., Garnier, J.M., Zheng, Y., Bottero, J.Y., 2004. Decoupling of as and Fe release to Bangladesh groundwater under reducing conditions. Part II: evidence from sediment incubations. Geochim. Cosmochim. Acta 68, 3475—3486.

Wang, Y.X., Shvartsev, S.L., Su, C.L., Evans, W.C., Harmon, R.S., Wanty, R.B., 2009. Genesis of arsenic/fluoride-enriched soda water: a case study at Datong, northern China. Appl. Geochem. 24, 641—649.

Wang, Y., Xie, X., Johnson, T.M., Lundstrom, C.C., Ellis, A., Wang, X., Duan, M., Li, J., 2014. Coupled iron, sulfur and carbon isotope evidences for arsenic enrichment in groundwater. J. Hydrol 519, 414—422.

Welch, A.H., Lico, M.S., 1998. Factors controlling As and U in shallow ground water, southern Carson Desert, Nevada. Appl. Geochem. 13, 521—539.

WHO, 2011. Guideline for Drinking-water Quality, fourth ed. World Health Organ-ization.Geneva, Switzerland, p. 564.

Wilkin, R.T., Wallschläger, D., Ford, R.G., 2003. Speciation of arsenic in sulfidic waters. Geochem. Trans. 4, 1—7.

Wilkin, R.T., Ford, R.G., 2006. Arsenic solid-phase partitioning in reducing sedi-ments of a contaminated wetland. Chem. Geol. 228, 156—174.

Xie, X., Ellis, A., Wang, Y., Xie, Z., Duan, M., Su, C., 2009. Geochemistry of redox-sensitive elements and sulfur isotopes in the high arsenic groundwater sys-tem of Datong Basin, China. Sci. Total Environ. 407, 3823—3835.

Xie, X., Wang, Y., Su, C., Li, J., Li, M., 2012. Influence of irrigation practices on arsenic mobilization: evidence from isotope composition and Cl/Br ratios in ground-water from Datong Basin, northern China. J. Hydrol 424, 37—47.

Xie, X., Wang, Y., Ellis, A., Li, J., Su, C., Duan, M., 2013a. Multiple isotope (O, S and C) approach elucidates the enrichment of arsenic in the groundwater from the Datong Basin, northern China. J. Hydrol 498, 103—112.

Xie, X., Johnson, T.M., Wang, Y., Lundstrom, C.C., Ellis, A., Wang, X., Duan, M., 2013b. Mobilization of arsenic in aquifers from the Datong Basin, China: evidence from

geochemical and iron isotopic data. Chemosphere 90 (6), 1878–1884.

Zhang, J., Ma, T., Feng, L., Yan, Y., Abass, O.K., Wang, Z., Cai, H., 2017. Arsenic behavior in different biogeochemical zonations approximately along the groundwater flow path in Datong Basin, northern China. Sci. Total Envion 584, 458–468.

Zhang, D., Guo, H., Xiu, W., Ni, P., Zheng, H., Wei, C., 2017. In-situ mobilization and transformation of iron oxides-adsorbed arsenate in natural groundwater.

J. Hazard Mater. 321, 228–237.

Zhou, Y., Zeng, Y., Zhou, J., Guo, H., Li, Q., Jia, R., Chen, Y., Zhao, J., 2017. Distribution of groundwater arsenic in Xinjiang, P. R. China. Appl. Geochem. 77, 116–125.

Zobrist, J., Dowdle, P.R., And, J.A.D., Oremland, R.S., 2000. Mobilization of arsenite by dissimilatory reduction of adsorbed arsenate. Environ. Sci. Technol. 34, 4747–4753.